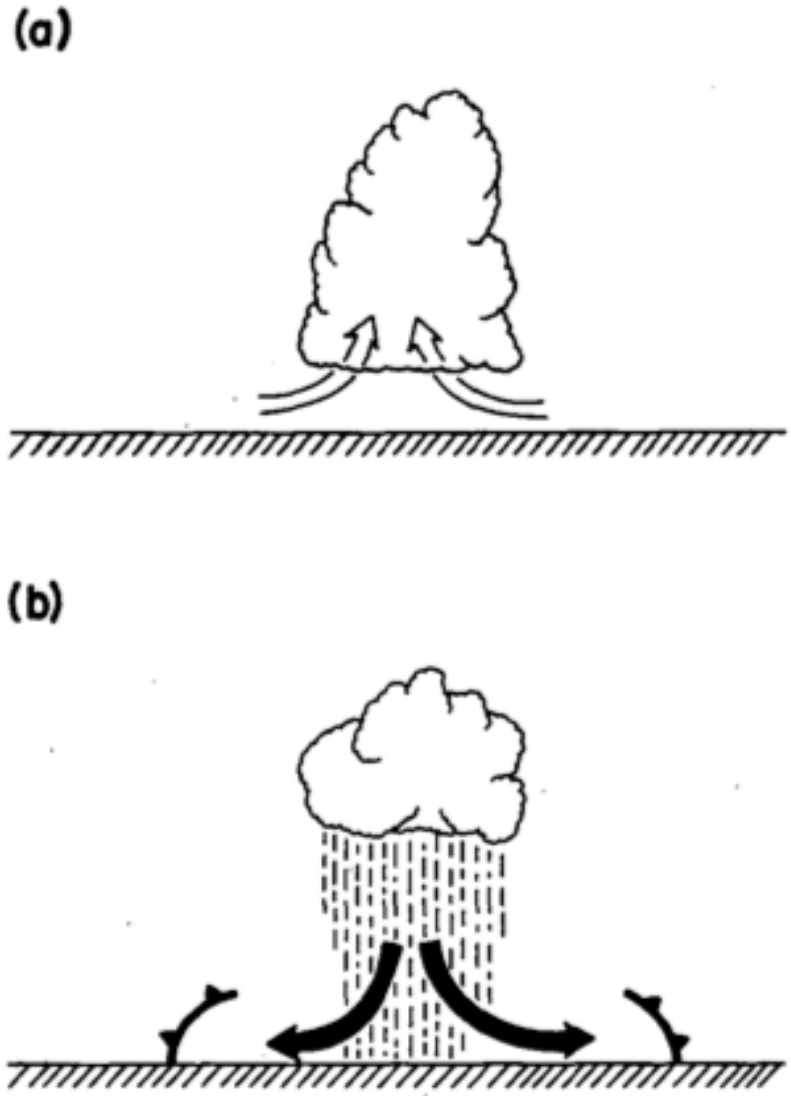

FIG. 1. Schematic illustration of the life cycle of an ordinary thunderstorm cell in which the (a) initial updraft, yields to a (b) downdraft produced by the accumulation of rain within the updraft. (Adapted from Figs. 17–18 of Byers and Braham, 1949.)

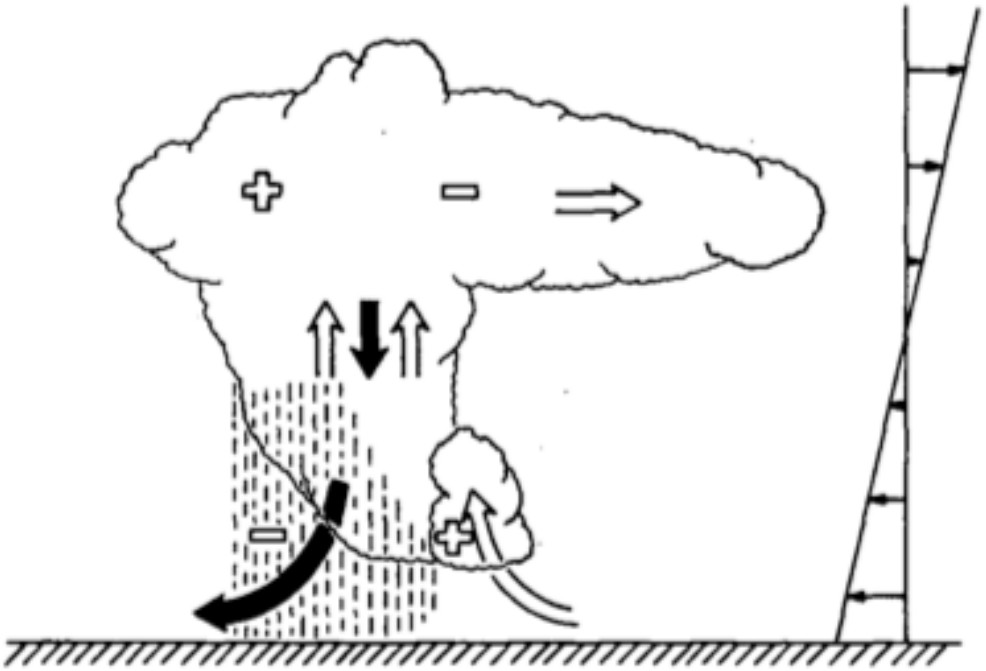

FIG. 2. Newton's proposal that a system of updrafts and downdrafts acts to reduce the shear within the squall line and thus produce a convergence/divergence pattern (indicated by the open plus and minus signs, respectively) which favors new growth downshear of the existing line. (Adapted from Fig. 16 of Newton, 1950.)

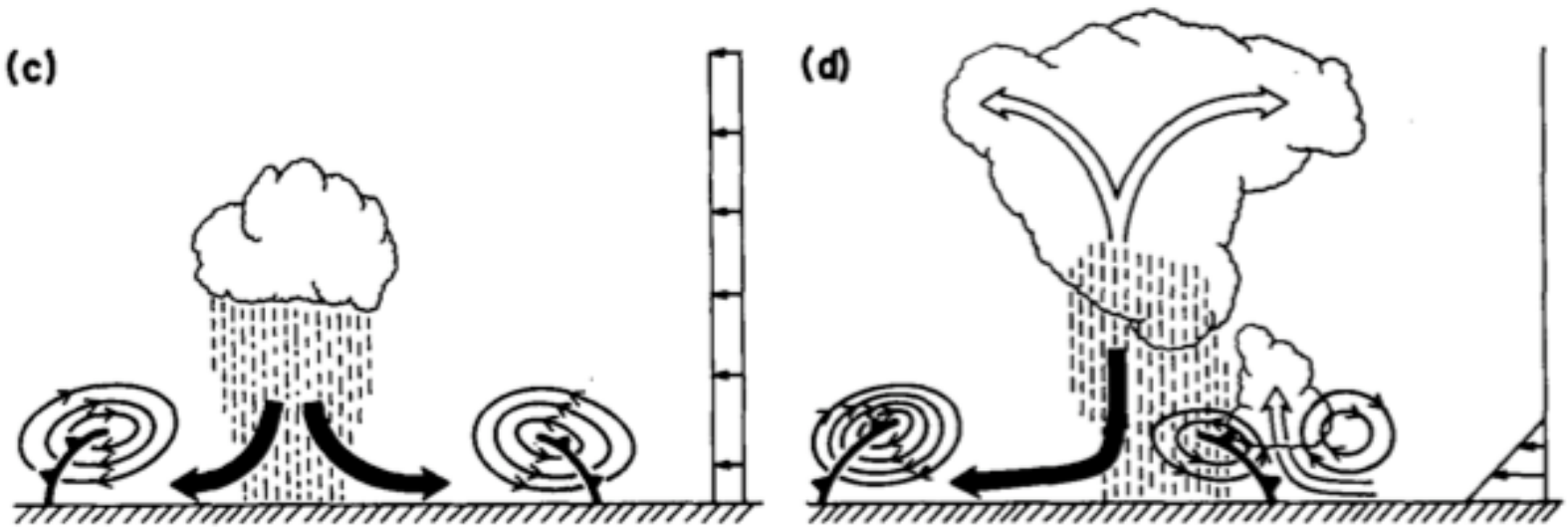

FIG. 5. Thorpe, et al. (1982, pp. 741–743) argue that (a) without low-level shear, the rain-produced cold pool propagates away from the cloud above and that the shear at the top of the pool dissipates new cells triggered by the cold pool, whereas (b) with low-level shear, the cold pool remains beneath the cloud and produces a long-lived cell. In the present study, we argue that (c) without low-level shear, the circulation of a spreading cold pool inhibits deep lifting and so cannot trigger a cell. (d) The presence of low-level shear counteracts the circulation of the cold pool and promotes deep lifting that triggers new cells.

RKW Theory

Rotunno, Klemp, and Weisman

(1988): A theory for long-lived squall lines.

J. Atmos. Sci., **45,** 463 – 485.

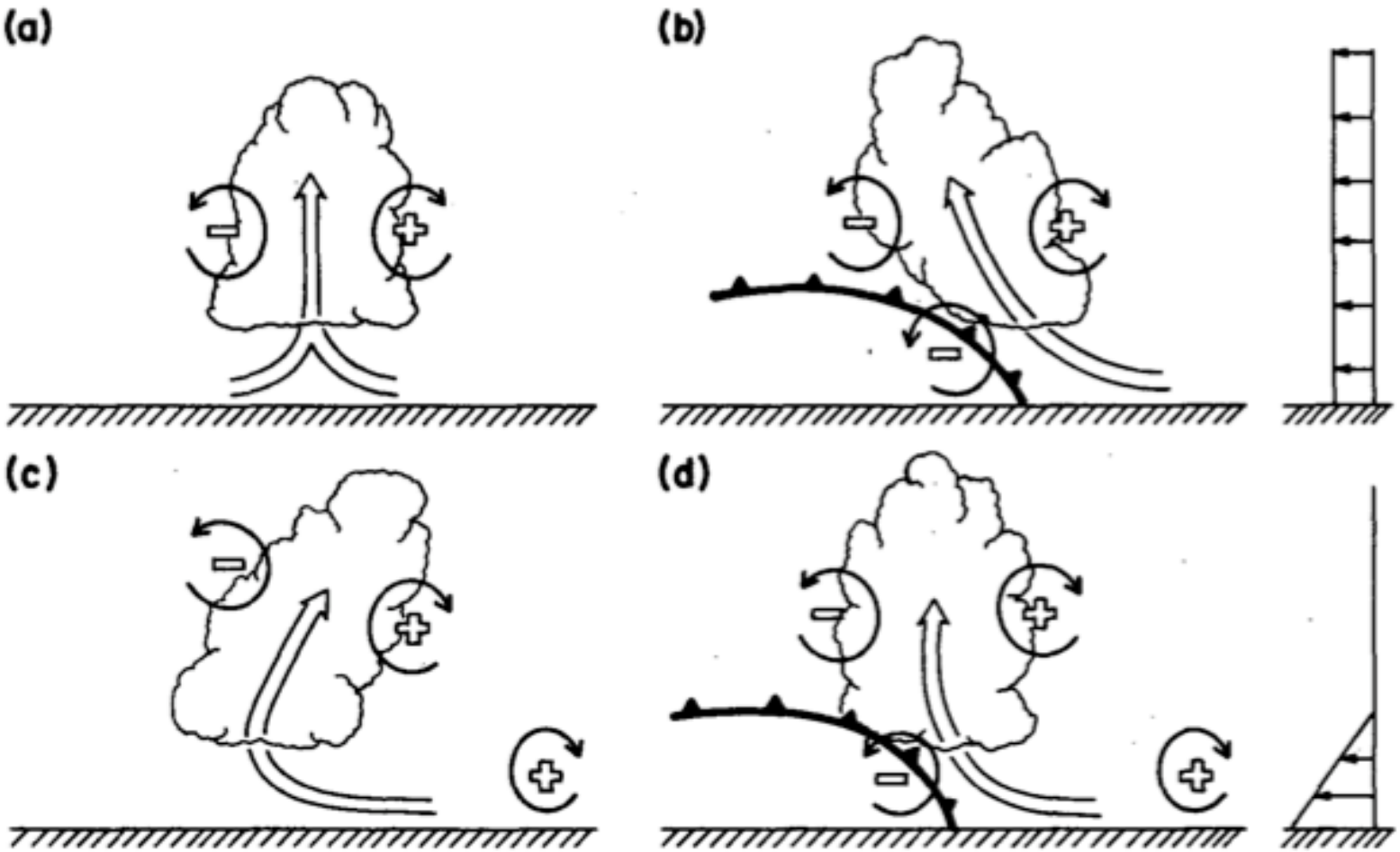

FIG. 18. Schematic diagram showing how a buoyant updraft may be influenced by wind shear and/or a cold pool. (a) With no shear and no cold pool, the axis of the updraft produced by the thermally created, symmetric vorticity distribution is vertical. (b) With a cold pool, the distribution is biased by the negative vorticity of the underlying cold pool and causes the updraft to lean upshear. (c) With shear, the distribution is biased toward positive vorticity and this causes the updraft to lean back over the cold pool. (d) With both a cold pool and shear, the two effects may negate each other, and allow an erect updraft.

RKW 1988

RKW 1988

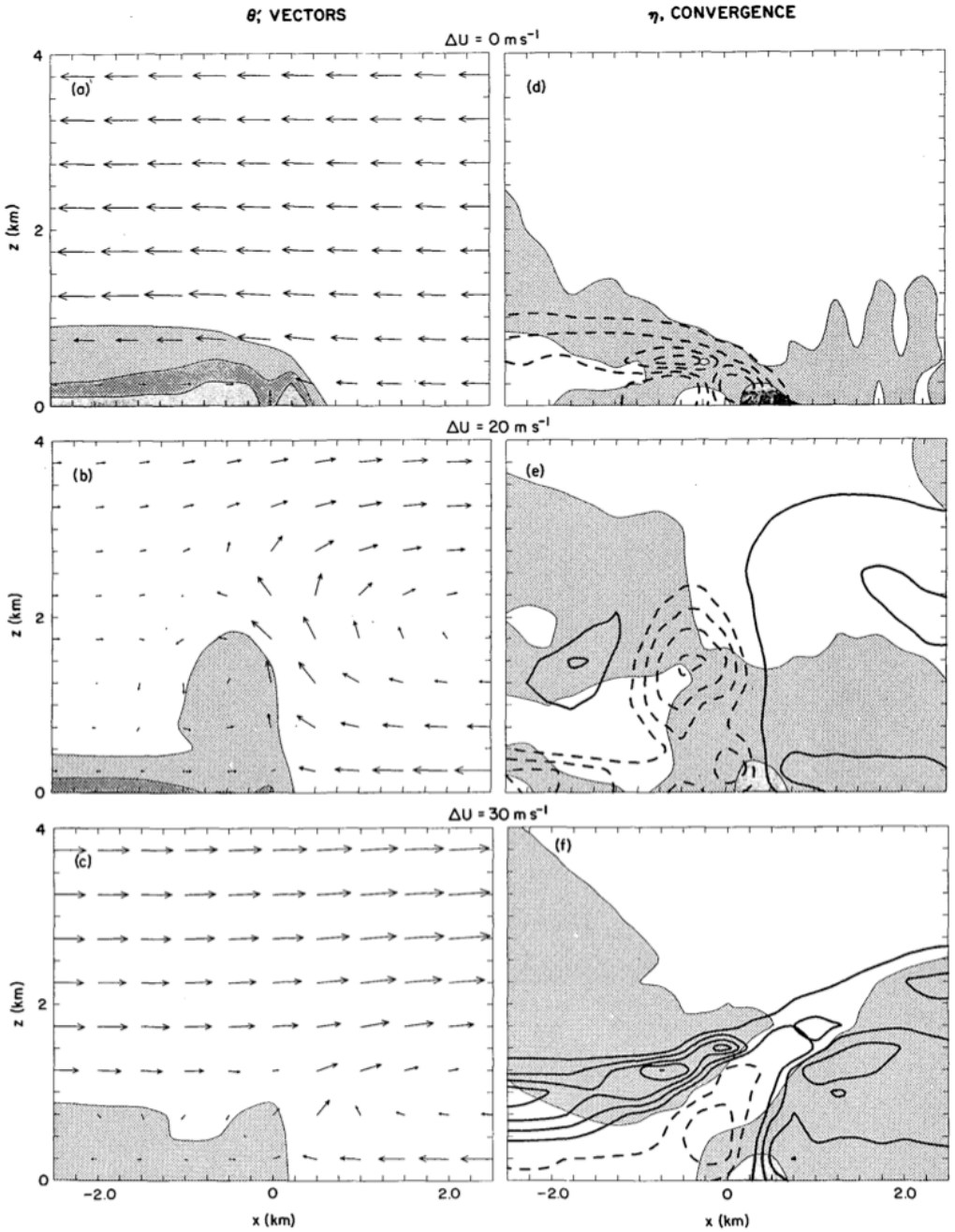

FIG. 20. The spreading cold pool at t = 15 min for ΔU = 0, 20 and 30 m s^{-1}. In (a)–(c), cold pool-relative vectors are plotted at every other grid point (2 grid lengths represents 15 m s^{-1}). The negative potential temperature perturbations are shaded at 2 K intervals, beginning at −1 K. In (d)–(f), η is contoured in intervals of 0.005 s^{-1} (negative values dashed, zero line not shown). Areas of positive convergence are lightly shaded and areas where the convergence exceeds 0.01 s^{-1} are darkly shaded. Convergence is less than 0.016 s^{-1} in all cases.

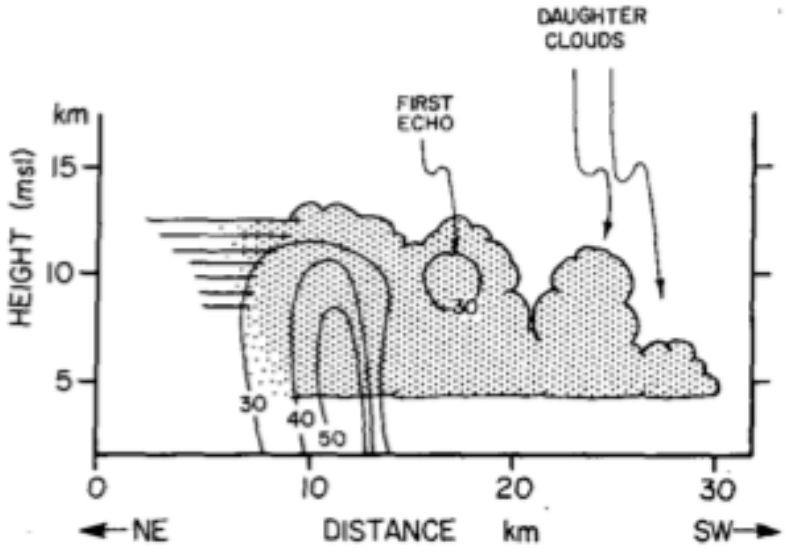

FIG. 1. Schematic diagram showing an NE-SW cross section through a typical hailstorm of western South Dakota. Stippled shading denotes cloud; solid contours represent radar reflectivity in dBz (adapted from Dennis *et al.*, 1970).

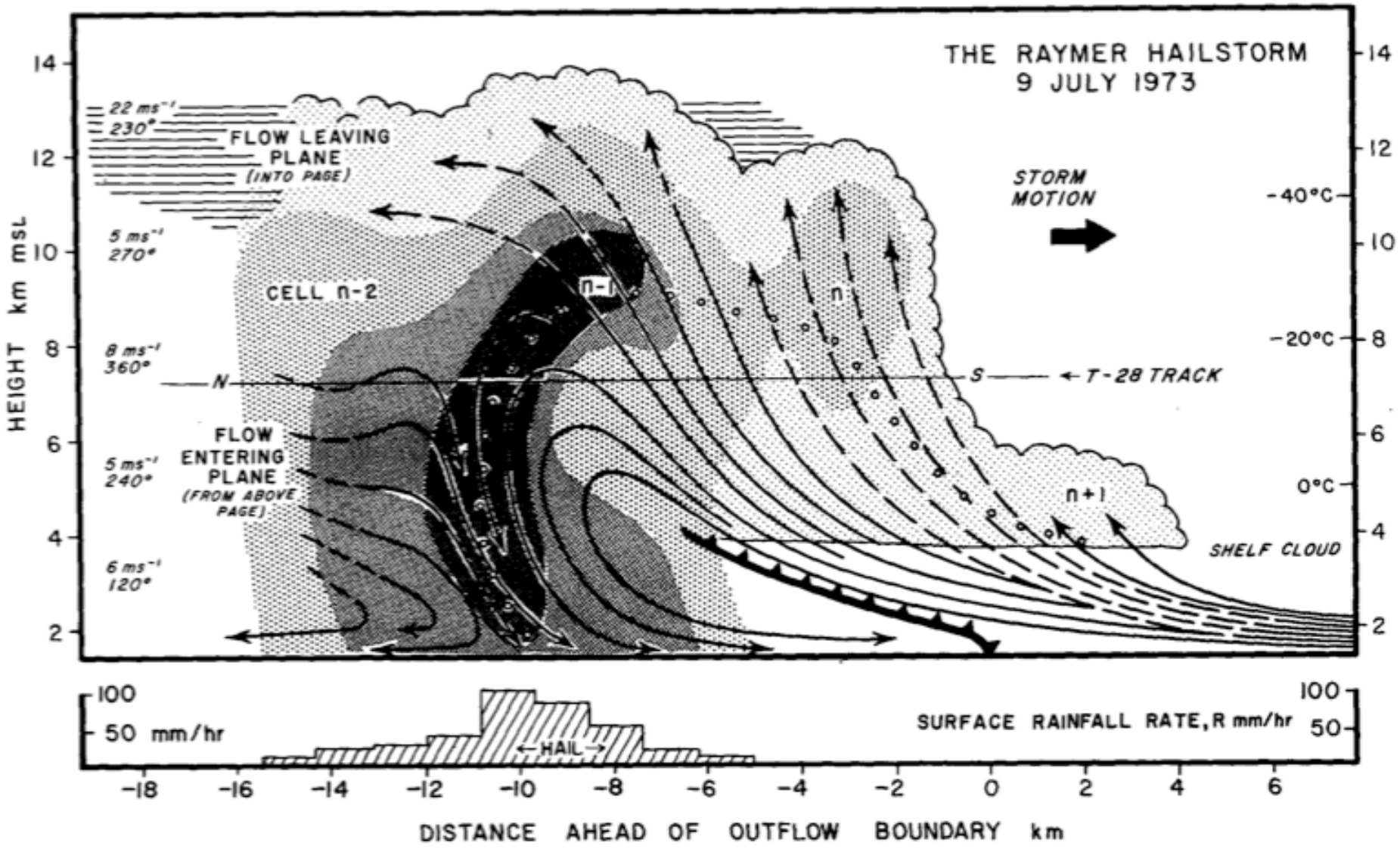

Browning et al. 1976

TABLE 2. Statistics concerning mature phase repeat cycles.

Low-level shear (Δu) (m s^{-1}/2.5 km)	Time between first echoes (min)	Secondary cells per cycle	Average period between cells (min)
5.0	~12	0	~12
7.5	16	0	16
10.0	32 or 16	1 or 0	16
12.5	36	1	18
15.0	40	1	20
17.5	40	1	20
20.0	43	1 or 2	22 or 14
22.5	∞	(all)	17
(25.0)	∞	(all)	17
(27.5)	∞	(all)	17
(30.0)	∞	(all)	15

Fovell and Ogura 1989

Fovell and Tan 1998a

TABLE 1. Mature phase summary statistics for some simulations from the shear-layer depth experiment.

Shear-layer depth (km)	Note	Storm speed average (m s^{-1})	Fundamental period of oscillation (min)	Repeat cycle length–number of cells per cycle (min)	Mode of temporal behavior	Stability of temporal behavior
1.66	(1)	12.3	12.5	not applicable	Aperiodic	Persistent
2.00	(1)	13.5	15.4	not applicable	Aperiodic	Persistent
2.25	(2)	14.7	15.2	15.2/1	Simply periodic	Transitional
2.50		15.1	15.0	15.0/1	Simply periodic	Persistent
3.00		16.0	14.3	14.3/1	Simply periodic	Persistent
3.75	(3)	16.7	13.8	13.8/1	Simply periodic	Transitional
3.75	(4)	16.2	14.1	28.2/2	Complex periodic	Transitional
5.00		16.4	13.8	27.6/2	Complex periodic	Persistent
6.25	(5)	16.9	13.6	27.2/2	Complex periodic	Persistent
7.50	(5)	17.2	13.4	26.8/2	Complex periodic	Persistent
8.00	(6)	17.5	13.4	26.8/2	Complex periodic	Persistent
8.25	(7)	16.6	13.8	27.6/2	Complex periodic	Transitional
8.25	(8)	17.4	12.8	12.8/1	Simply periodic	Transitional
8.75		16.6	13.8	13.8/1	Simply periodic	Persistent
10.00		16.5	13.6	13.6/1	Simply periodic	Persistent

Notes: (1) No fundamental period. Cell period shown is average separation period during mature phase. Estimates are very unstable. (2) After transition at around 350 minutes. (3) For time $t < 400$ minutes. (4) For time $400 < t < 700$ minutes. (5) Possibly aperiodic case. (6) Persistent after transition around 300–400 minutes. (7) For time $400 < t < 600$ minutes. Possibly aperiodic during this time. See Fig. 11c. (8) For time $t > 600$ minutes. Nearly simply periodic during this time. See Fig. 11c.

Fovell and Tan 1998b

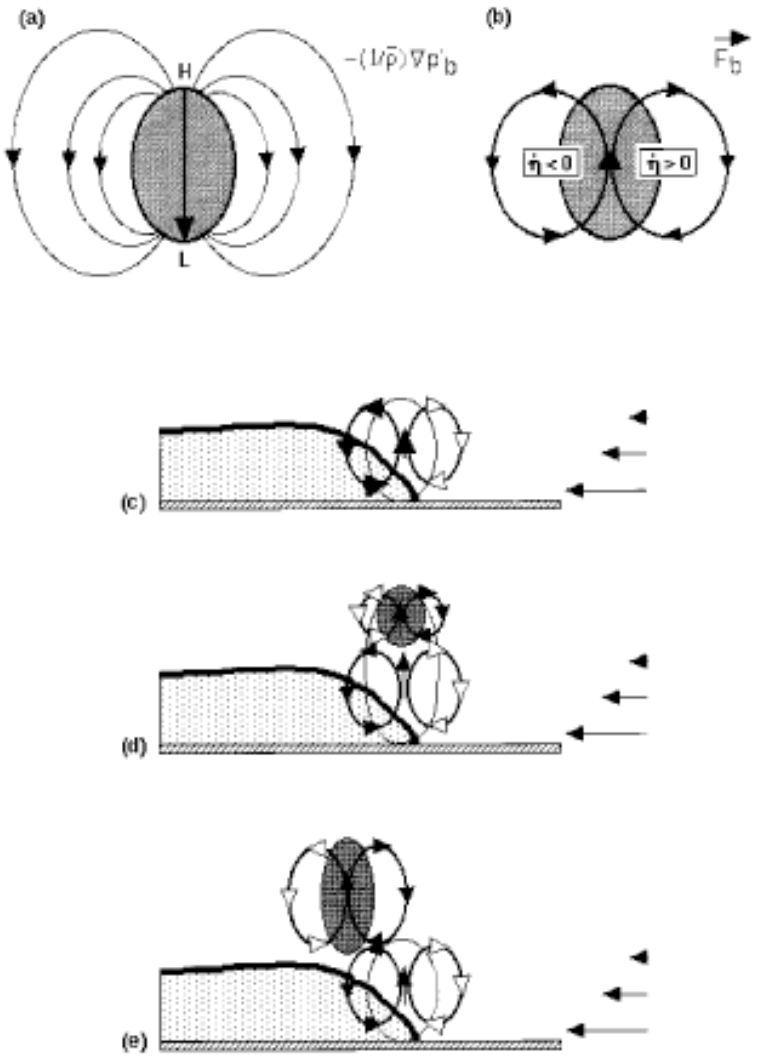

FIG. 10. Schematic illustrating the effect of an individual convective cell on the storm's low-level circulation (see text). Panel (a) shows the BPGA vector field associated with a finite, positively buoyant parcel, while (b) shows the full $\mathbf{F}_b$ field and the circulatory tendency associated with baroclinic vorticity generation $\dot{\eta}$. Panel (c) presents RKW's analysis of the circulation tendency at the subcloud cold pool (stippled region) boundary. Panel (d) adds a positively buoyant region with its attendant circulatory tendency, illustrating the initial formation of a convective cell. Panel (e) shows the cell's effect at a subsequent time.

Fovell and Tan 1998a

Three stages in life cycle of a convective cell

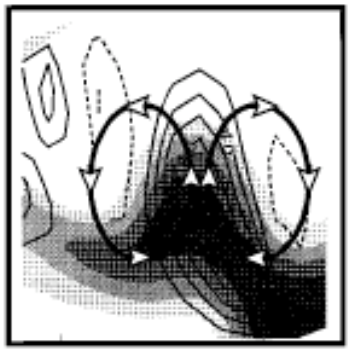

Stage 1 (initiation of cell)

Buoyancy-induced circulation helps new cell rise, strengthen. Potentially warm air ingested from below.

Rise of cell establishes ribbon of potentially warm air in FTR airflow emanating from low-level storm inflow.

Stage 2 (maturation of cell)

Growing cell's buoyancy-induced circulation acts to weaken forced lifting, reduce potentially warm inflow.

Stable, potentially cold air mixes into cell's inflow from wake beneath, eroding its convective instability.

Cell's original, least diluted air concentrated near top of updraft. In 3D simulation, cell dynamically splits.

Stage 3 (dissipation of cell)

Cell's buoyancy-induced circulation on front-facing flank weakens as mixing erodes instability. Cell "splinters" and disorganizes.

During disorganization, original, least diluted air effectively "detrained" from splintered updraft, spreading about (above and to sides) of updraft shown. In consequence, on rear-facing side, buoyancy-induced circulation acts to dissipate rear-facing flank of updraft, slowing cell's rearward propagation.

FIG. 16. The three stages of a convective cell. Equivalent potential temperature (shaded) and vertical velocity (contoured) fields were taken from Fig. 3. Note the reference, frame shown is not fixed in space, but rather tracks the cell's principal updraft.

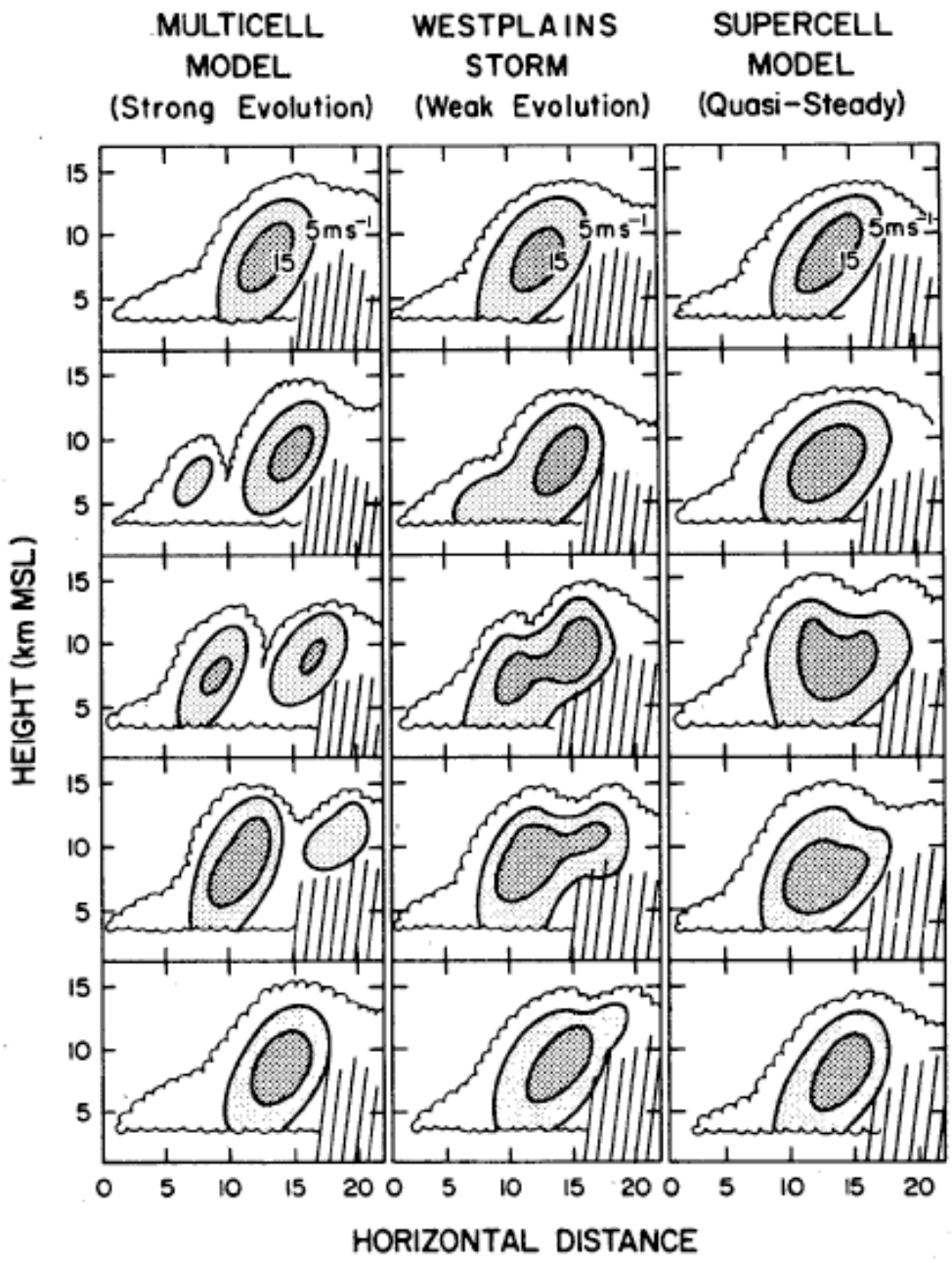

FIG. 17. Schematic diagram showing updraft evolution for three different storm models. Contours represent isotachs of vertical wind speed. Time between successive frames, moving down the figure, is meant to be 3–5 min. Reproduced from Foote and Frank (1983).

1) *The supercell storm.* It consists of one large cell (supercell) which propagates continuously to the right of the mean winds. The radar echo very often contains a hook near cloud base height.
2) *The multi-cell storm.* It consists of several cells which are laterally aligned. Discrete propagation occurs on the right flank. The individual cells move through the storm complex and dissipate on the left flank. Three subclasses of multi-cell storms were identified: the individual cells propagate to the left of the mean environmental winds, the individual cells move with the environmental winds, or the individual cells propagate to the right of the environmental winds.
3) *The severely sheared storm.* It consists of one large cell (and bounded WER). An instantaneous view of this storm with a PPI radar indicates that it is a supercell storm. Observations over a longer period of time suggest that it evolves in a steadily changing manner such that discrete propagation occurs on the front flank at intervals of the order of one hour. (This class has been identified only tentatively since just two cases are really well documented.)
4) *The squall line.* It consists of laterally aligned cells which do not disruptively interfere with one another nor compete for the available low level warm moist air. Individual cells are equal in intensity and may last for several hours (cf. Newton, 1963).

Marwitz 1972c

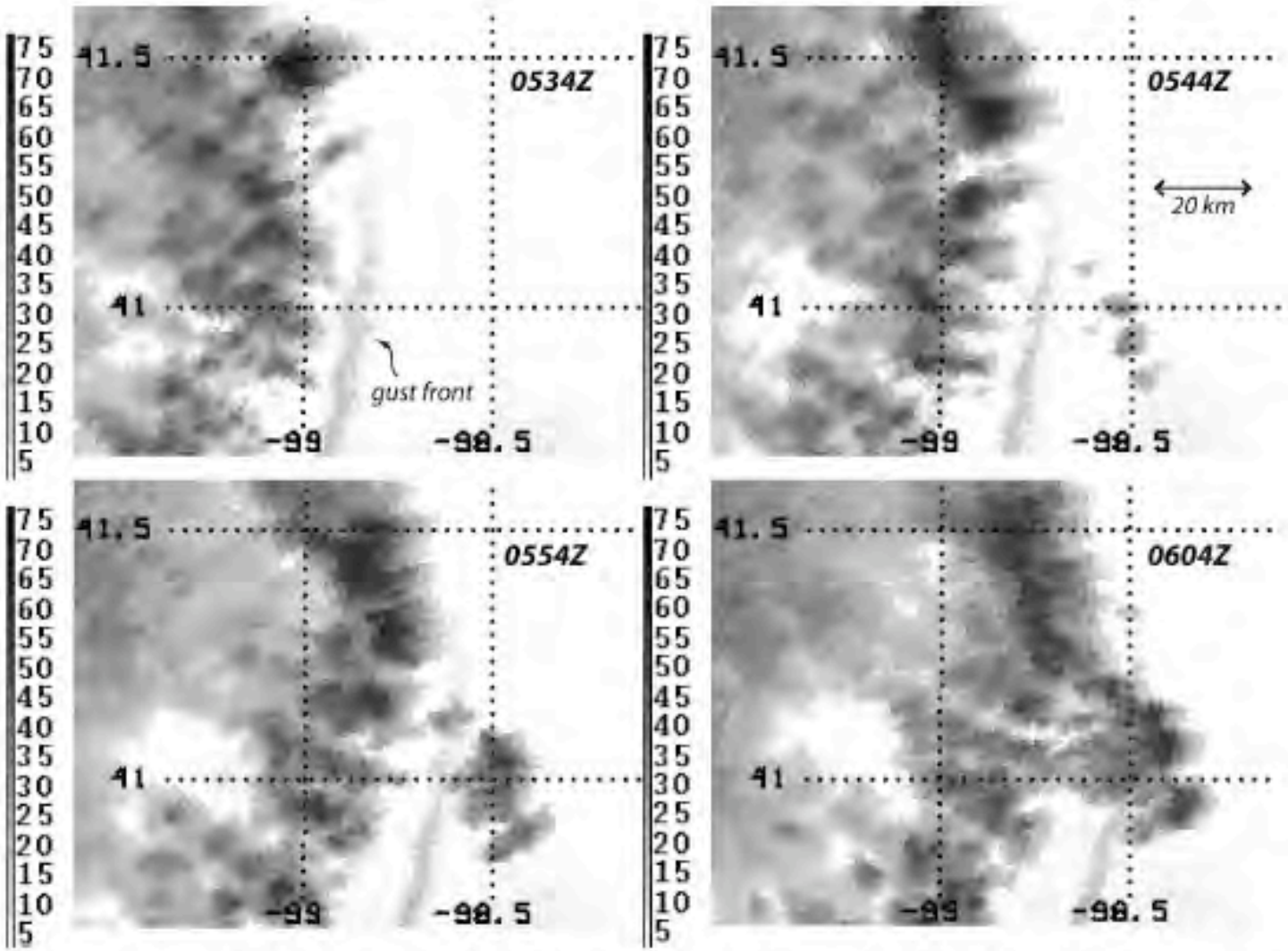

FIG. 1. Hastings, NE, Next-Generation Weather Radar (NEXRAD) imagery from 8 Jul 2003, showing radar reflectivity with superposed latitude and longitude markers.

Fovell et al. 2006

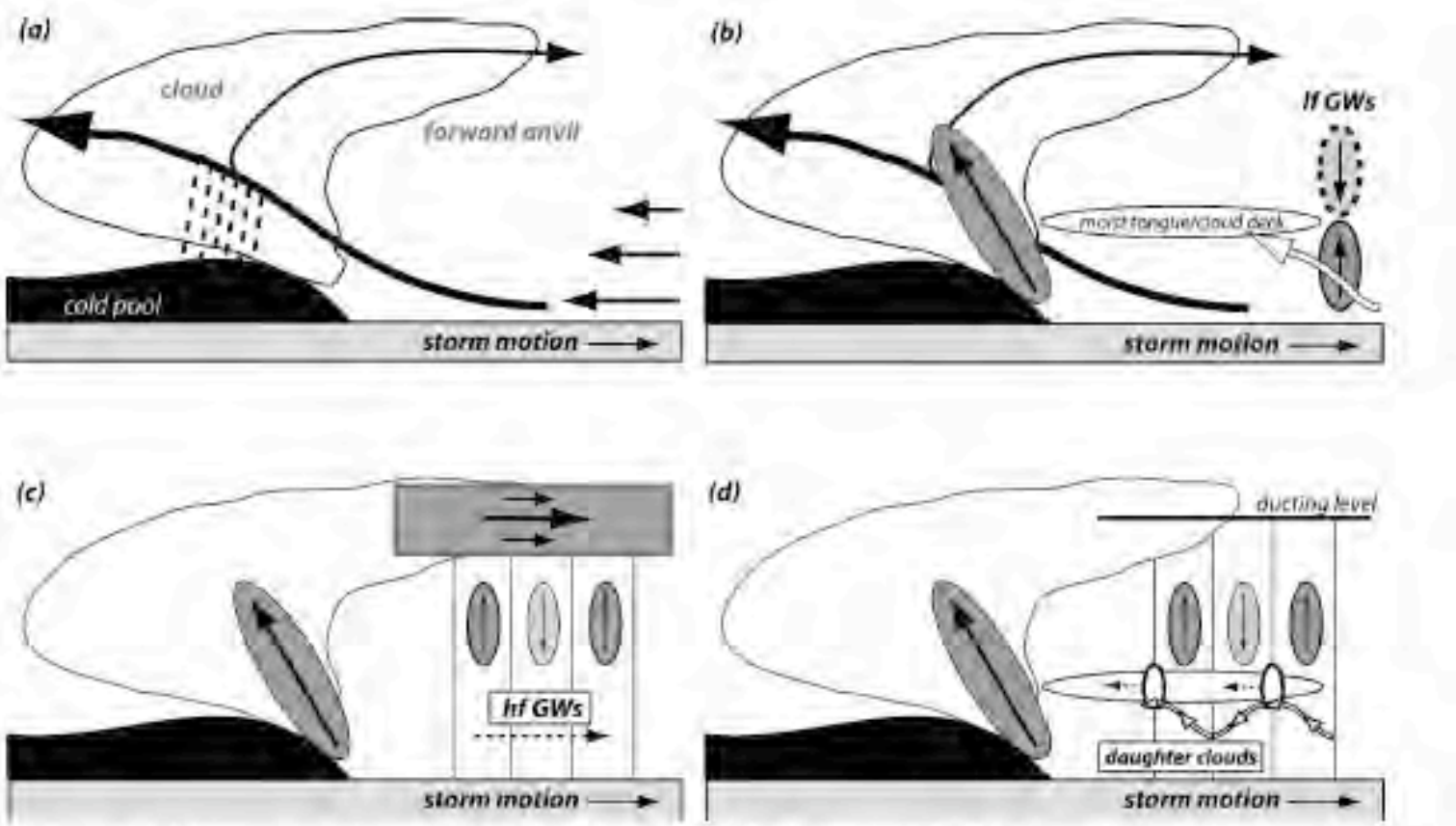

FIG. 16. Schematic description of the factors involved in the forward CI and discrete propagation events discussed in this study. See text for further information.

Fovell et al. 2006